A Generalized Local Binary Pattern Operator for Multiresolution Gray Scale and Rotation Invariant Texture Classification

Timo Ojala, Matti Pietikäinen and Topi Mäenpää
Machine Vision and Media Processing Unit
Infotech Oulu, University of Oulu
P.O.Box 4500, FIN - 90014 University of Oulu, Finland
{skidi, mkp, topiolli}@ee.oulu.fi
http://www.ee.oulu.fi/research/imag/texture

Abstract. This paper presents generalizations to the gray scale and rotation invariant texture classification method based on local binary patterns that we have recently introduced. We derive a generalized presentation that allows for realizing a gray scale and rotation invariant LBP operator for any quantization of the angular space and for any spatial resolution, and present a method for combining multiple operators for multiresolution analysis. The proposed approach is very robust in terms of gray scale variations, since the operator is by definition invariant against any monotonic transformation of the gray scale. Another advantage is computational simplicity, as the operator can be realized with a few operations in a small neighborhood and a lookup table. Excellent experimental results obtained in a true problem of rotation invariance, where the classifier is trained at one particular rotation angle and tested with samples from other rotation angles, demonstrate that good discrimination can be achieved with the occurrence statistics of simple rotation invariant local binary patterns. These operators characterize the spatial configuration of local image texture and the performance can be further improved by combining them with rotation invariant variance measures that characterize the contrast of local image texture. The joint distributions of these orthogonal measures are shown to be very powerful tools for rotation invariant texture analysis.

nonparametric texture analysis distribution histogram Brodatz contrast

1 Introduction

Most approaches to texture classification assume, either explicitly or implicitly, that the unknown samples to be classified are identical to the training samples with respect to spatial scale, orientation and gray scale properties. However, real world textures can occur at arbitrary spatial resolutions and rotations and they may be subjected to varying illumination conditions. This has inspired a collection of studies, which generally incorporate invariance with respect to one or at most two of the properties spatial scale, orientation and gray scale, among others [1,2,3,4,5,6,7,8,10,11,13,14].

This work focuses on gray scale and rotation invariant texture classification, which has been addressed by Chen and Kundu [2] and Wu and Wei [13]. Both studies approached gray scale invariance by assuming that the gray scale transformation is a linear function. This is a somewhat strong simplification, which may limit the usefulness of the proposed methods. Chen and Kundu realized gray scale invariance by glo-

bal normalization of the input image using histogram equalization. This is not a general solution, however, as global histogram equalization can not correct intraimage (local) gray scale variations.

Recently, we introduced a theoretically and computationally simple approach for gray scale and rotation invariant texture analysis based on Local Binary Patterns, which is robust in terms of gray scale variations and discriminated rotated textures efficiently [8,10]. A novel contribution of this paper is the generalized presentation of the operator that allows for realizing it for any quantization of the angular space and for any spatial resolution. We derive the operator for a general case based on a circularly symmetric neighbor set of P members on a circle of radius R. We call this operator $LBP_{P,R}^{riu2}$. P controls the quantization of the angular space, whereas R determines the spatial resolution of the operator. In addition to evaluating the performance of individual operators of a particular (P,R), we also propose a straightforward approach for multiresolution analysis, which combines the information provided by multiple operators.

The proposed operator $LBP_{P,R}^{riu2}$ is an excellent measure of the spatial structure of local image texture, but it by definition discards the other important property of local image texture, contrast, since it depends on the gray scale. If the stability of the gray scale is not a concern, the performance of $LBP_{P,R}^{riu2}$ can be further enhanced by combining it with a rotation invariant variance measure $VAR_{P,R}$ that characterizes the contrast of local image texture. We present the joint distribution of these two complementary operators, $LBP_{P,R}^{riu2}/VAR_{P,R}$, as a powerful tool for rotation invariant texture classification. The proposed operators are also computationally attractive, as they can be realized with a few operations in a small neighborhood and a lookup table.

The performance of the proposed approach is demonstrated with an image data used in a recent study on rotation invariant texture classification [11]. Excellent experimental results demonstrate that our texture representation learned at a specific rotation angle generalizes to other rotation angles.

The paper is organized as follows. The operators, the classification principle and a simple method for multiresolution analysis are described in Section 2. Experimental results are presented in Section 3 and Section 4 concludes the paper.

2 Methodology

2.1 Generalized Rotation Invariant LBP Operator

We start the derivation of our gray scale and rotation invariant texture operator by defining texture T in a local neighborhood of a monochrome texture image as the joint distribution of gray levels $\{g_c, g_0, ..., g_{P-1}\}$ (P>1). The gray value g_c corresponds to the gray value of the center pixel of the local neighborhood and g_p (p=0,...,$P-1$) correspond to the gray values of P equally spaced pixels on a circle of radius R (R>0) that form the circularly symmetric neighbor set $N(P,R)$. If the coordinates of g_c are $(0,0)$, then the coordinates of g_p are given by $(-R\sin(2\pi p/P), R\cos(2\pi p/P))$. For brevity we omit the derivation presented in [8], and obtain the following generalized operator for gray scale and rotation invariant texture description:

$$LBP_{P,R}^{riu2} = \begin{cases} \sum_{p=0}^{P-1} s(g_p - g_c) & \text{if } U(N(P,R)) \le 2 \\ P+1 & \text{otherwise} \end{cases} \quad (2)$$

where

$$s(x) = \begin{cases} 1, x \ge 0 \\ 0, x < 0 \end{cases} \quad (3)$$

and

$$U(N(P,R)) = \left|s(g_{P-1} - g_c) - s(g_0 - g_c)\right| + \sum_{p=1}^{P-1} \left|s(g_p - g_c) - s(g_{p-1} - g_c)\right| \quad (4)$$

Invariance against any monotonic transformation of the gray scale is achieved by considering the signs of the differences $s(g_p-g_c)$, which effectively corresponds to binary thresholding of the local neighborhood, hence the expression *L*ocal *B*inary *P*attern. Rotation invariance is achieved by recognizing that a set of rotation variant patterns originates from a particular rotation invariant pattern upon rotation.

Uniformity measure *U* corresponds to the number of spatial transitions, i.e. bitwise 0/1 changes between successive bits in the circular representation of the *LBP*. We argue that the larger the uniformity value *U* is, i.e. the larger number of spatial transitions occurs in the pattern, the more likely the pattern is to change to a different pattern upon rotation in digital domain. Based on this argument we designate those rotation invariant patterns that have *U* value of at most 2 as 'uniform', and use the occurrence statistics of different 'uniform' patterns for texture discrimination.

By definition exactly *P*+1 'uniform' binary patterns can occur in a circularly symmetric neighbor set of *P* pixels. Eq.(2) assigns an unique label to each of them, the label corresponding to the number of '1' bits in the pattern (0->*P*), while the 'nonuniform' patterns are grouped under the miscellaneous label *P*+1. The selection of 'uniform' patterns with the simultaneous compression of 'nonuniform' patterns is also supported by the fact that the former tend to dominate in deterministic textures [8]. In practice the computation of $LBP_{P,R}^{riu2}$, which has *P*+2 distinct output values, is best implemented with a lookup table of 2^P elements.

The expression in Eq.(2) allows generalizing the operator for any quantization of the angular space and for any spatial resolution. The quantization of the angular space is defined by ($360^o/P$). However, certain considerations have to be taken into account in the selection of *P* and *R*. First, they are related in the sense that for a given *R*, additional new elements placed on the circle are not likely to provide any useful information beyond a certain point. Second, an efficient implementation with a lookup table of 2^P elements sets a practical upper limit for *P*.

2.2 Rotation Invariant Variance Measures of Texture Contrast

The $LBP_{P,R}^{riu2}$ operator is a truly gray scale invariant measure, i.e. its output is not affected by any monotonic transformation of the gray scale. It is an excellent measure

of the spatial pattern, but it by definition discards contrast. If we under stable lighting conditions wanted to incorporate the contrast of local image texture as well, we can measure it with a rotation invariant measure of local variance:

$$VAR_{P,R} = \frac{1}{P}\sum_{p=0}^{P-1}(g_p - \mu)^2 \qquad \text{, where } \mu = \frac{1}{P}\sum_{p=0}^{P-1} g_p \tag{5}$$

$VAR_{P,R}$ is by definition invariant against gray scale shifts. Since $LBP_{P,R}^{riu2}$ and $VAR_{P,R}$ are complementary, their joint distribution $LBP_{P,R}^{riu2}/VAR_{P,R}$ is expected to be a very powerful rotation invariant measure of local image texture. Note that even though we in this study restrict ourselves to using only joint distributions of $LBP_{P,R}^{riu2}$ and $VAR_{P,R}$ operators that have the same (P,R) values, nothing would prevent us from using joint distributions of operators with different neighborhoods.

2.3 Nonparametric Classification Principle

In the classification phase a test sample S was assigned to the class of the model M that maximized the log-likelihood measure:

$$L(S, M) = \sum_{b=1}^{B} S_b \log M_b \tag{6}$$

where B is the number of bins, and S_b and M_b correspond to the sample and model probabilities at bin b, respectively. This nonparametric (pseudo-)metric measures likelihoods that samples are from alternative texture classes, based on exact probabilities of feature values of pre-classified texture prototypes. In the case of the joint distribution $LBP_{P,R}^{riu2}/VAR_{P,R}$, the log-likelihood measure was extended in a straightforward manner to scan through the two-dimensional histograms.

Sample and model distributions were obtained by scanning the texture samples and prototypes with the chosen operator, and dividing the distributions of operator outputs into histograms having a fixed number of B bins. Since $LBP_{P,R}^{riu2}$ has a completely defined set of discrete output values (0 -> P+1), no additional binning procedure is required, but the operator outputs are directly accumulated into a histogram of P+2 bins. Variance measure $VAR_{P,R}$ has a continuous-valued output, hence quantization of its feature space is needed, together with the selection of an appropriate value for B [9].

2.4 Multiresolution Analysis

By altering P and R we can realize our operators for any quantization of the angular space and for any spatial resolution. Multiresolution analysis can be accomplished by combining the information provided by multiple operators of different (P,R). In this study we perform straightforward multiresolution analysis by defining the aggregate

(dis)similarity as the sum of individual log-likelihoods computed for individual operators:

$$L_O = \sum_{o=1}^{O} L(S^o, M^o) \quad (7)$$

where O is the number of operators, and S^o and M^o correspond to the sample and model histograms extracted with operator o (o=1,...,O), respectively.

3 Experiments

We demonstrate the performance of our operators with imagery used in a recent study on rotation invariant texture classification by Porter and Canagarajah [11]. They presented three feature extraction schemes for rotation invariant texture classification, employing the wavelet transform, a circularly symmetric Gabor filter and a Gaussian Markov Random Field with a circularly symmetric neighbor set. They concluded that the wavelet-based approach was the most accurate and exhibited the best noise performance, having also the lowest computational complexity.

We first replicate the original experimental setup as carefully as possible, to get comparable results. Since in the original setup the training data included samples from several rotation angles, we also present results for a more challenging setup, where the samples of just one particular rotation angle are used for training the texture classifier, which is then tested with the samples of the other rotation angles. In each case we report as the result the error rate, i.e. the percentage of misclassified samples of all samples in the testing data, for the individual operators $LBP_{P,R}^{riu2}$ and $VAR_{P,R}$, and their joint distribution $LBP_{P,R}^{riu2}/VAR_{P,R}$.

Regarding the selection of P and R, in order to incorporate three different spatial resolutions and three different angular resolutions we chose to realize $LBP_{P,R}^{riu2}$ and $VAR_{P,R}$ with (P,R) values of (8,1), (16,2), and (24,3). In multiresolution analysis we use the three 2-resolution combinations and the one 3-resolution combination these three alternatives can form. Regarding the quantization of the continuous $VAR_{P,R}$ feature space, histograms contained 128 bins when $VAR_{P,R}$ operator was used by itself, and (P+2)/16 bins in the case of the joint $LBP_{P,R}^{riu2}/VAR_{P,R}$ operator.

3.1 Image Data and Experimental Setup

Image data included 16 texture classes from the Brodatz album shown in Fig. 1. For each texture class there were eight 256x256 images, of which the first was used for training the classifier, while the other seven images were used to test the classifier. Rotated textures had been created from these source images using a proprietary interpolation program that produced images of 180x180 pixels in size. If the rotation angle was a multiple of 90 degrees (0^o or 90^o in the case of present ten rotation angles), a small amount of artificial blur had been added to the original images to simulate the

effect of blurring on rotation at other angles [11].

In the original experimental setup the texture classifier was trained with several 16x16 subimages extracted from the training image. This fairly small size of training samples increases the difficulty of the problem nicely. The training set comprised rotation angles 0^o, 30^o, 45^o, and 60^o, while the textures for classification were presented at rotation angles 20^o, 70^o, 90^o, 120^o, 135^o, and 150^o. Consequently, the test data included 672 samples, 42 (6 angles x 7 images) for each of the 16 texture classes. Using a Mahalanobis distance classifier Porter and Canagarajah reported 95.8% accuracy for the rotation invariant wavelet-based features as the best result.

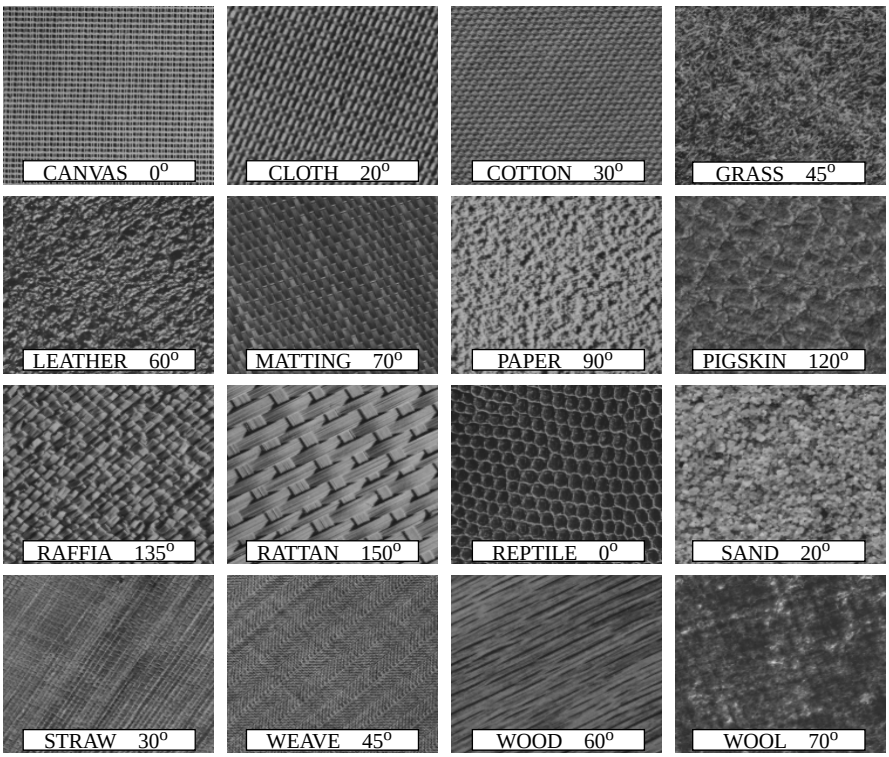

Fig. 1. Texture images printed at particular orientations.

3.2 Experimental Results

We started replicating the original experimental setup by dividing the 180x180 images of the four training angles (0^o, 30^o, 45^o, and 60^o) into 121 disjoint 16x16 subimages. In other words we had 7744 training samples, 484 (4 angles x 121 samples) in each of the 16 texture classes. We first computed the histogram of the chosen operator for each of the 16x16 samples. We then added the histograms of all samples belonging to a particular class into one big model histogram for this class, since the histograms of single 16x16 samples would have been too sparse to be reliable models. Also, using 7744 dif-

ferent models would have resulted in computational overhead, for in the classification phase the sample histograms were compared to every model histogram. Consequently, we obtained 16 reliable model histograms containing $484(16\text{-}2R)^2$ entries (the operators have a R pixel border). The performance of the operators was evaluated with the 672 testing images. Corresponding sample histograms contained $(180\text{-}2R)^2$ entries, hence we did not have to worry about their stability.

Table 1: Error rates (%) for the original experimental setup, where training is done with rotations 0^o, 30^o, 45^o, and 60^o.

P,R	$LBP_{P,R}^{riu2}$	$VAR_{P,R}$	$LBP_{P,R}^{riu2}/VAR_{P,R}$
8,1	11.76	4.46	1.64
16,2	1.49	11.61	0.15
24,3	0.89	13.39	3.57
8,1+16,2	1.04	1.34	0.30
8,1+24,3	0.45	1.64	0.00
16,2+24,3	1.04	12.05	0.89
8,1+16,2+24,3	0.89	3.42	0.00

Classification results are given in Table 1. As expected, $LBP_{16,2}^{riu2}$ and $LBP_{24,3}^{riu2}$ clearly outperformed their simpler counterpart $LBP_{8,1}^{riu2}$. $LBP_{8,1}^{riu2}$ had difficulties in discriminating strongly oriented textures, as misclassifications of *rattan*, *straw* and *wood* contributed 70 of the 79 misclassified samples. Interestingly, in all 79 cases the model of the true class ranked second right after the most similar model of a false class that led to misclassification. $LBP_{16,2}^{riu2}$ did much better, classifying all samples correctly except ten *grass* samples that were assigned to *leather.* Again, in all ten cases the model of the true class ranked second. $LBP_{24,3}^{riu2}$ provided further improvement by missing just five *grass* samples and a *matting* sample. In all six cases the model of the true class again ranked second. These results demonstrate that the 45^o quantization of the angular space by $LBP_{8,1}^{riu2}$ is too crude.

Combining the $LBP_{P,R}^{riu2}$ operator with the $VAR_{P,R}$ operator, which did not too badly by itself, generally improved the performance. The lone exception was (24,3) where the addition of the poorly performing $VAR_{24,3}$ only hampered the excellent discrimination by $LBP_{24,3}^{riu2}$. We see that $LBP_{16,2}^{riu2}/VAR_{16,2}$ fell one sample short of a faultless result, as a *straw* sample at 90^o angle was labeled as *grass.* The error rates for single resolutions are so low that there is not much room for improvement by the multiresolution analysis, though two alternatives of the joint distribution provided a perfect classification. The largest gain was achieved for the $VAR_{P,R}$ operator, especially when $VAR_{24,3}$ was excluded.

Even though a direct comparison to the results of Porter and Canagarajah may not

be meaningful due to the different classification principle, the excellent results for our operators demonstrate their suitability for rotation invariant texture classification.

Table 2 presents results for a more challenging experimental setup, where the classifier was trained with samples of just one rotation angle and tested with samples of other nine rotation angles. We trained the classifier with the 121 16x16 samples extracted from the designated training image, again merging the histograms of the 16x16 samples of a particular texture class into one model histogram. The classifier was tested with the samples obtained from the other nine rotation angles of the seven source images reserved for testing purposes, totaling 1008 samples, 63 in each of the 16 texture classes. Note that in each texture class the seven testing images are physically different from the one designated training image, hence this setup is a true test for the texture operators' ability to produce a rotation invariant representation of local image texture that also generalizes to physically different samples.

Table 2: Error rates (%) when training is done at just one rotation angle, and the average error rate over the ten angles.

OPERATOR	***P,R***	**TRAINING ANGLE**										**AVERAGE**
		0°	**20°**	**30°**	**45°**	**60°**	**70°**	**90°**	**120°**	**135°**	**150°**	
$LBP^{riu2}_{P,R}$	8,1	31.3	13.6	15.3	23.6	15.0	15.7	30.6	15.6	23.7	15.2	19.94
	16,2	3.8	1.0	1.4	1.1	1.5	0.9	2.4	1.4	1.3	2.5	1.72
	24,3	1.3	1.1	0.9	2.4	0.8	1.8	0.0	1.3	3.3	2.0	1.48
	8,1+16,2	5.7	0.5	0.2	0.2	1.5	2.8	7.1	0.4	0.8	0.8	1.99
	8,1+24,3	3.8	0.4	0.6	1.4	0.6	1.1	2.8	0.5	1.7	0.6	1.34
	16,2+24,3	2.3	0.0	0.2	0.8	0.7	0.0	0.4	0.6	1.5	1.6	0.80
	8,1+16,2+24,3	2.4	0.0	0.0	0.8	0.0	0.0	1.5	0.0	1.4	0.2	0.63
$VAR_{P,R}$	8,1	7.3	3.4	5.4	6.0	4.4	3.1	6.1	5.8	5.4	4.4	5.10
	16,2	10.1	15.5	13.8	9.5	12.7	14.4	9.0	10.2	9.2	11.5	11.60
	24,3	14.6	13.6	14.3	15.6	14.6	14.4	14.0	13.3	13.7	14.1	14.21
	8,1+16,2	2.5	3.1	1.2	1.0	2.1	2.3	2.5	0.9	1.2	2.1	1.88
	8,1+24,3	4.8	3.0	1.3	1.1	2.5	1.5	3.9	0.5	1.0	2.1	2.15
	16,2+24,3	11.7	13.5	13.2	13.1	14.5	13.5	10.7	13.1	12.5	12.9	12.87
	8,1+16,2+24,3	5.1	5.4	3.0	1.7	3.8	3.8	5.0	1.8	1.9	2.7	3.39
$LBP^{riu2}_{P,R}/VAR_{P,R}$	8,1	0.9	5.8	4.3	2.7	4.8	5.6	0.7	4.0	2.7	4.4	3.56
	16,2	0.0	0.5	0.6	0.6	0.6	0.4	0.0	0.5	0.5	0.3	0.40
	24,3	4.2	5.0	3.8	2.6	4.0	4.5	4.4	2.8	2.1	2.1	3.52
	8,1+16,2	0.0	0.7	0.9	0.8	0.7	0.8	0.0	0.7	0.7	0.6	0.59
	8,1+24,3	0.2	0.2	0.4	0.2	0.4	0.2	0.4	0.3	0.2	0.1	0.26
	16,2+24,3	2.8	1.1	1.1	0.2	0.4	0.1	2.7	0.4	0.2	0.1	0.90
	8,1+16,2+24,3	0.0	0.3	0.5	0.2	0.4	0.3	0.2	0.4	0.2	0.1	0.26

Training with just one rotation angle allows a more conclusive analysis of the rotation invariance of our operators. For example, it is hardly surprising that $LBP_{8,1}^{riu2}$ provides highest error rates when the training angle is a multiple of 45^o. Due to the crude quantization of the angular space the presentations learned at 0^o, 45^o, 90^o, or 135^o do not generalize that well to other angles. Again, the importance of the finer quantization of the angular space shows, as $LBP_{16,2}^{riu2}$ and $LBP_{24,3}^{riu2}$ provide a solid performance with average error rates of 1.72% and 1.48%, respectively. Even though the results for multiresolution analysis generally exhibit improved discrimination over single resolutions, they also serve as a welcome reminder that the addition of inferior operator does not necessarily enhance the performance.

4 Discussion

We presented a theoretically and computationally simple yet efficient multiresolution approach to gray scale and rotation invariant texture classification based on local binary patterns and nonparametric discrimination of sample and prototype distributions. We derived a generalized presentation that allows for realizing the gray scale and rotation invariant operator $LBP_{P,R}^{riu2}$ for any quantization of the angular space and for any spatial resolution, and proposed a method for multiresolution analysis.

The proposed approach is very robust in terms of gray scale variations, since the $LBP_{P,R}^{riu2}$ operator is by definition invariant against any monotonic transformation of the gray scale. This should make it very attractive in situations where varying illumination conditions are a concern, e.g. in visual inspection. Gray scale invariance is also necessary if the gray scale properties of the training and testing data differ. This was clearly demonstrated in our recent study [9] on supervised texture segmentation with the same the image set that was used by Randen and Husoy in their recent extensive comparative study [12]. However, real world textures with a large tactile dimension can also exhibit non-monotonic intensity changes, e.g. due to moving shadows, which neither our approach nor any other 2-D texture operator tolerates.

We achieved rotation invariance by recognizing that the LBP operator encodes a set of rotation invariant patterns. An interesting alternative to obtain rotation invariant features would be to carry out 1-D Fourier transform on the circularly symmetric neighbor set [1].

We showed that the performance can be further enhanced by multiresolution analysis. We presented a straightforward method for combining operators of different spatial resolutions for this purpose. Experimental results involving three different spatial resolutions showed that multiresolution analysis is beneficial, except in those cases where a single resolution was already sufficient for a very good discrimination. Ultimately, we would want to incorporate scale invariance, in addition to gray scale and rotation invariance.

We also reported that when there are classification errors, the model of the true class very often ranks second. This suggests that classification could be carried out in stages, by selecting features which best discriminate among remaining alternatives.

Acknowledgments

The authors wish to thank Dr. Nishan Canagarajah and Mr. Paul Hill from the University of Bristol for providing the texture images used in this study. The financial support provided by the Academy of Finland is gratefully acknowledged.

Note

The source code and the texture images used in this study, together with other imagery used in our published work, can be downloaded from *http://www.ee.oulu.fi/research/imag/texture*.

References

1. Arof H and Deravi F. Circular neighbourhood and 1-D DFT features for texture classification and segmentation. IEE Proc. - Vision, Image and Signal Processing 1998; 145:167-172.
2. Chen J-L and Kundu A. Rotation and gray scale transform invariant texture identification using wavelet decomposition and hidden Markov model. IEEE Trans. Pattern Analysis and Machine Intelligence 1994; 16:208-214.
3. Cohen FS, Fan Z and Patel MA. Classification of rotated and scaled texture images using Gaussian Markov Random Field models. IEEE Trans. Pattern Analysis and Machine Intelligence 1991; 13:192-202.
4. Fountain SR and Tan TN. Efficient rotation invariant texture features for content-based image retrieval. Pattern Recognition 1998; 31:1725-1732.
5. Haley GM and Manjunath BS. Rotation-invariant texture classification using a complete space-frequency model. IEEE Trans. Image Processing 1999; 8:255-269.
6. Kashyap RL and Khotanzad A. A model-based method for rotation invariant texture classification. IEEE Trans. Pattern Analysis and Machine Intelligence 1986; 8:472-481.
7. Lam W-K and Li C-K. Rotated texture classification by improved iterative morphological decomposition. IEE Proc. - Vision, Image and Signal Processing 1997; 144:171-179.
8. Ojala T, Pietikäinen M & Mäenpää T. Gray scale and rotation invariant texture classification with Local Binary Patterns. Proc. Sixth European Conference on Computer Vision, Dublin, Ireland, 2000; 1:404-420.
9. Ojala T, Valkealahti K, Oja E and Pietikäinen M. Texture discrimination with multidimensional distributions of signed gray level differences. Pattern Recognition 2000; 34(3), in press.
10. Pietikäinen M, Ojala T and Xu Z. Rotation-invariant texture classification using feature distributions. Pattern Recognition 2000; 33:43-52.
11. Porter R and Canagarajah N. Robust rotation-invariant texture classification: wavelet, Gabor filter and GMRF based schemes. IEE Proc. - Vision, Image and Signal Processing 1997; 144:180-188.
12. Randen T and Husoy JH. Filtering for texture classification: a comparative study. IEEE Trans. Pattern Analysis and Machine Intelligence 1999; 21:291-310.
13. Wu W-R and Wei S-C. Rotation and gray-scale transform-invariant texture classification using spiral resampling, subband decomposition and Hidden Markov Model. IEEE Trans. Image Processing 1996; 5:1423-1434.
14. You J and Cohen HA. Classification and segmentation of rotated and scaled textured images using texture 'tuned' masks. Pattern Recognition 1993; 26:245-258.